

Research Paper

The Effects of Milling on the Surface Properties of Form I Paracetamol Crystals

Jerry Y. Y. Heng,¹ Frank Thielmann,² and Daryl R. Williams^{1,2,3}

Received March 2, 2006; accepted April 18, 2006

Purpose. The effects of milling and particle size on surface energies of form I paracetamol crystals are reported.

Methods. Paracetamol crystals (75–850 μm) were obtained by cooling methanol and acetone saturated solutions. Additionally, macroscopic (>2 cm) single crystals were grown by slow solvent evaporation from saturated solutions, ball milled and sieved into different particle size fractions. Surface properties were characterised using Inverse Gas Chromatography and compared with those calculated from sessile drop contact angle measurements on macroscopic single crystals.

Results. Dispersive surface energies, γ_{SV}^d for milled samples increased by 20% with decreasing particle size. With decreasing particle size acceptor numbers, K_A values were constant but donor numbers, K_B decreased. For unmilled materials K_B was comparable to K_A but with a significantly lower γ_{SV}^d of only 33 mJ/m^2 . Milling resulted in fracture along the crystal's lowest attachment energy plane (010), exposing facets of different surface chemistry to that of the native external facets. θ for the (010) fracture plane confirmed a higher γ_{SV}^d compared to external facets such as (011) of single crystals.

Conclusions. Milling exposes a hydrophobic surface for paracetamol form I crystals which becomes increasingly more dominant with decreasing particle size.

KEY WORDS: habit; inverse gas chromatography; milling; particle size; surface energy.

INTRODUCTION

The surface properties of materials are of both fundamental and practical importance in the performance of particulate materials such as pharmaceutical and fine chemicals. In the case of pharmaceuticals, these properties can help predict processing stability, adhesion, colloid stability, agglomeration, powder flow and dissolution rates which in turn directly relate to product design and performance (1–3). However, until a comprehensive understanding of the solid state surface properties is available for these classes of materials, the ability to engineer surface properties for optimised product manufacture and performance will remain an elusive goal.

Milling is a commonly used unit operation employed for particle size reduction in many industries for a wide range of reasons (4). In the pharmaceutical industry, in the case of materials used for inhalation, milling is the preferred processing route for particle manufacture due to the relative difficulty in directly producing the required particle size in the crystallisation reactor. Milling may also often be used to create particles with enhanced dissolution properties due to their larger surface areas. It is common industrial practise

that materials that are milled, are subsequently processed by wet granulation.

The surface physicochemical properties of solids can be significantly governed by their surface energetics. Unlike liquid surfaces, the explicit experimental determination of the surface energy of solids is not easily achieved. The normal practise is to use indirect methods involving known gases, liquids or solids, which are placed in contact with the solid surface to be characterised. Most commonly, a solid's surface energy, γ_{SV}^d is obtained by measuring the contact angle of a reference liquid, of a known surface tension, with the unknown surface. The contact angle, θ , is the angle between the solid surface and the tangent of the liquid drop surface, through the liquid phase at the three phase (solid–liquid–vapour) contact point, and is related to the surface energy of the solid via the Young-Dupré equation (5) (1):

$$W_A = \gamma_{LV}(1 + \cos \theta) + \pi_e \quad (1)$$

where W_A is the solid–liquid work of adhesion, γ_{LV} is the liquid–vapour surface tension and π_e is the equilibrium spreading pressure for the liquid's vapour adsorbed onto the solid surface.

Inverse gas chromatography (IGC) is a simple, yet versatile and robust technique for studying the physicochemical properties of particulate and fibrous materials. This technique was first developed in the 1950s, and early work focused on characterisation of catalysts, adsorbents and polymers (6–9). IGC is simply the inverse use of a conven-

¹Department of Chemical Engineering, Imperial College London, South Kensington Campus, London, SW7 2AZ, UK.

²Surface Measurement Systems Ltd., 5 Wharfside, Rosemount Road, London, HA0 4PE, UK.

³To whom correspondence should be addressed. (e-mail: d.r.williams@imperial.ac.uk)

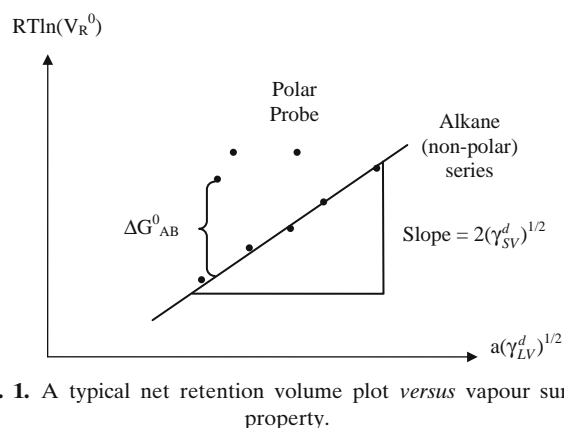


Fig. 1. A typical net retention volume plot versus vapour surface property.

tional gas chromatography (GC), in which a column is packed with an *unknown* solid sample and *known* vapour probes are injected into the column via an inert carrier gas. The retention time of the probe molecules is recorded by a GC detector, allowing the retention volume and then the partitioning co-efficient for the solid–vapour interaction to be determined. From this primary data, a wide range of physicochemical properties of solid materials such as surface energies, acid-base functionality of surfaces, diffusion kinetics, solubility parameters, surface heterogeneity and phase transition temperatures may be determined (10).

IGC has been shown to be a versatile and robust technique as exemplified by the increasing wide scope and range of applications. These include the characterisation of pharmaceutical solids, such as batch to batch variations, effects of milling, crystal habits, optical forms, production routes and effects of humidity on material properties (11–16). These references are reviewed in detail elsewhere (17). This information could be used to evaluate performance or stability of products as well as suitability of pharmaceutical delivery systems (18).

The net retention volume, V_R^o which is a fundamental surface thermodynamic property of the solid–vapour interaction process, is given by:

$$V_R^o = \frac{j}{m} \cdot F \cdot (t_R - t_o) \cdot \frac{T}{273.15} \quad (2)$$

where T is the column temperature in Kelvin (K), F is the carrier gas exit flow rate at standard temperature and pressure (STP), t_R is the retention time for adsorbing probe and t_o is the mobile phase hold-up time (dead-time), m is the sample mass in the packed column and j is the James-Martin correction, which corrects the retention time for the pressure drop along the column bed.

According to Fowkes (19), the work of adhesion between a solid and liquid is the summation of geometric mean terms of each component (dispersive and polar, if made up of dipole–dipole interactions). Owens-Wendt extended the Fowkes approach by grouping the terms into dispersive and polar components as shown in Eq. 3:

$$W_A = 2 \cdot \sqrt{\gamma_{LV}^d \cdot \gamma_{SV}^d} + 2 \cdot \sqrt{\gamma_{LV}^p \cdot \gamma_{SV}^p} \quad (3)$$

Though, a more contemporary formalism would be to consider the dispersive interactions as Lifshitz-van der Waals interactions, and the polar interactions as acid-base interactions. Using IGC, where a series of non-polar ($\gamma_{LV}^p = 0$) probes are used, the free energy of adsorption can be expressed by:

$$RT \ln V_R^o = 2N_A \cdot a \cdot \sqrt{\gamma_{LV}^d \cdot \gamma_{SV}^d} + K \quad (4)$$

The dispersive component of a solid, γ_{SV}^d as described by Schultz *et al.* (20), can be determined by plotting $RT \ln (V_R^o)$ versus $a(\gamma_{LV}^d)^{1/2}$. Dorris and Gray suggested a similar approach which took into account the contribution of a methylene group in the alkane series to the free energy of desorption (21). Surface energy results obtained using both methods are normally found to be very similar (22).

When using a polar probe such as ethanol, values of V_R^o may be considered to consist of a dispersive as well as an acid-base component. The acid-base component is also referred to as polar component or specific interactions and takes into account non-dispersive interactions. With a knowledge of γ_{LV}^d for the polar probes used, then the dispersive component of V_R^o may be plotted. Then the difference between the $RT \ln (V_R^o)$ values obtained and the dispersive line may be equated to the acid-base adsorption energy contribution, G_{AB}^o as shown in Fig. 1. This specific interaction of polar probes with known electron acceptor

Table I. Acid-Base Numbers of Probe Molecules Used in IGC

Probes	$a(\gamma_{LV}^d)^{1/2}$ [1] $\text{m}^2(\text{J}/\text{m}^2)^{1/2}$	DN [2] kJ/mol	AN* [3] kJ/mol
<i>n</i> -undecane	1.27×10^{-19}	–	–
<i>n</i> -decane	1.15×10^{-19}	–	–
<i>n</i> -nonane	1.04×10^{-19}	–	–
<i>n</i> -octane	9.19×10^{-20}	–	–
Ethanol	5.13×10^{-20}	79.80	43.26
Acetone	4.37×10^{-20}	71.40	10.50
Ethyl acetate	4.62×10^{-20}	71.82	6.30
Acetonitrile	3.56×10^{-20}	59.22	19.74
Dichloromethane	3.83×10^{-20}	0.00	16.38

[1] Values obtained from the SMS-iGC analysis software (version 1.2).

[2] Donor numbers according to Gutmann's.

[3] Acceptor numbers according to Fowkes'.

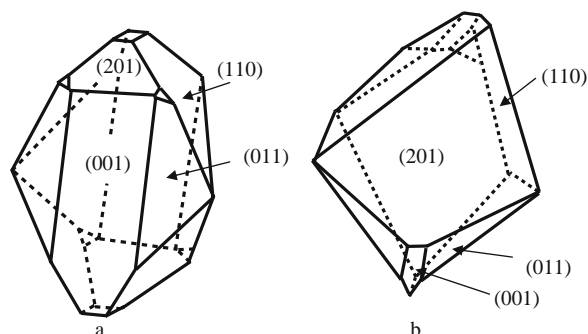


Fig. 2. Morphology of paracetamol crystal (a) Grown from methanol solution (b) Grown from acetone solution.

(AN) and electron donor (DN) numbers are used to evaluate the acid-base characteristics of the solid by Gutmann's semi-empirical relation (23) as follows:

$$-\Delta H_{AB}^o = AN \cdot K_B + DN \cdot K_A \quad (5)$$

where ΔH_{AB}^o is the enthalpy of interaction due to specific (acid-base) interactions between probe and solid surface, K_A is the acidity constant of the solid whilst K_B is the basicity constant of the solid. In this study, we used the corrected acceptor numbers AN^* proposed by Riddle and Fowkes (24) and these values are shown in Table I. The K_A and K_B constants of the solid surface are obtained from the slope and intercept, respectively, of the $\Delta H_{AB}^o/AN^*$ versus DN/AN^* plot.

Crystals are an assembly of rigid lattice of molecules, with regular internal structure resulting in smooth surfaces on crystals with characteristic shapes (25). Within the bulk crystal lattice, all available functional groups of the repeat molecule are involved in intramolecular or intermolecular interactions. However, on the surface of a crystal, some chemical groups will be free to interact with external molecules, be they solids, liquids or gases. In complex crystalline materials it is very likely that chemical groups on each crystal facet are dissimilar and thus have very different surface properties. It has been recently reported that the individual crystal facets of paracetamol form I exhibit anisotropic contact angle wettability and some significant variations in both dispersive and polar surface energy for facets (201), (001), (011) and (110) (26). These results were ascribed to variations in the surface hydroxyl group concentrations which were verified with XPS. As paracetamol is a complex organic compound, with functional groups of hydroxyl, carbonyl, amine and a benzene ring, the presence of both non-specific and specific interactions for the crystal surfaces is a reasonable expectation.

In this study, the surface energies of paracetamol form I as a function of particle size of fine (unmilled) single crystals and milled macroscopic crystals were investigated. The samples prepared were of single crystals grown from methanol and acetone saturated solutions giving rise to differing crystal habits as well as milled samples of macroscopic large crystals. These particulate materials were then characterised using IGC. Their surface energies were evaluated via IGC and compared with liquid sessile drop contact angle data on macroscopic single crystals.

MATERIALS AND METHODS

Materials

Paracetamol (4-acetamidophenol) obtained was >99% purity (Sigma-Aldrich, Poole, UK). The crystallisation solvents, methanol and acetone, were HPLC grade (Sigma-Aldrich, Poole, UK). IGC vapour probes were generated from HPLC grade undecane, decane, nonane, octane, ethanol, acetone, ethyl acetate, acetonitrile and dichloromethane obtained from Aldrich (Poole, UK). Contact angle probe liquids were deionised water, diiodomethane (>99%, Acros Organics, Belgium), formamide (>99.5%, Acros Organics, Belgium) and ethylene glycol (>99%, Sigma-Aldrich, Poole, UK). All chemicals were used without further purification except for diiodomethane, which was purified by passing through chromatographic columns of silica and (Merck, UK, Silica gel for column chromatography, 70–230 mesh) and basic alumina (Sigma-Aldrich, Dorset, UK, STD Grade, activated basic, 150 mesh) to remove any free iodine or any other contaminants present.

Preparation of Fine Paracetamol Crystalline Powder

Paracetamol powder was dissolved in methanol and acetone, respectively, for the preparation of saturated solutions at 15°C. These saturated solutions were then heated to 30°C and additional paracetamol was added until the solubility limit was reached. The warm solutions were then allowed to cool quickly to ambient room temperature, at a constant stirring rate. Seed crystals were added resulting in nucleation of a fine crystalline powder. These solutions were decanted and the solids dried by suction filtration. It was observed that the crystals nucleated from acetone saturated solutions favoured the formation of agglomerates as reported in literature (27).

These paracetamol powders were then sieved for 30 min using a test sieve shaker through a series of stainless steel test sieves (Pascall Engineering, Suffolk, UK). The following

Table II. Results of Advancing Contact Angles on Macroscopic Form I Paracetamol Crystals

Facet	Advancing contact angles, θ_a (degrees)			
	Diiodomethane	Water	Ethylene glycol	Formamide
(011)	50.7 ± 2.9	29.8 ± 5.7	10.9 ± 2.5	14.5 ± 2.5
(010)	27.8 ± 2.5	67.7 ± 2.5	42.5 ± 3.2	46.9 ± 2.4

Table III. Surface Energy Components of Macroscopic Form I Paracetamol Crystals Facets (011) and Cleaved Facet (010)

Facet	γ_{SV}^d	γ_{SV}^p	γ_{SV}^T	$\gamma_{SV}^p/\gamma_{SV}^T$
(011)	33.9	32.7	66.5	0.49
(010)	45.1	7.0	52.1	0.13

sieved fractions were obtained: 75–150, 150–250, 250–425, 425–600 and 600–825 μm .

Preparation of Macroscopic Paracetamol Crystals

Saturated methanol and acetone solutions were prepared at 20°C. A single seed crystal was suspended in the saturated solution without stirring on a single aramid fibre. Macroscopic (>2 cm) paracetamol single crystals were grown from saturated solutions by slow evaporation of solvent at 20°C over a period of 20–30 days. The macroscopic single crystal habits are shown in Fig. 2 and correspond to those reported previously in the literature (28). Crystals were dried under ambient conditions inside an empty beaker prior to conducting sessile drop contact angle measurements.

Preparation of Milled Paracetamol Crystals

Large macroscopic crystals grown from saturated solutions of methanol and acetone were milled with a ball-mill in a porcelain pot (Pascall Engineering, Suffolk, UK) with ceramic balls for 4 h. The resultant milled paracetamol powders were then sieved for 30 min using a test sieve shaker through a series of stainless steel test sieves (Pascall Engineering, Suffolk, UK). The following sieved fractions were obtained: 32–75, 75–125, 125–150, 150–250, 250–425 and 425–600 μm .

Inverse Gas Chromatography

Paracetamol powder was packed into pre-silanised glass columns (300 \times 4 mm ID) with silanised glass wool packing at each end. Prior to measurements samples were pre-treated at 303 K, 0% RH for 2 h under flowing helium to remove any residual moisture or solvent adsorbed on the powder surface. These samples were then loaded into a SMS-iGC 2000 (Surface Measurement Systems Ltd., London, UK) system. Following pre-treatment, pulse injections using a 0.25 ml gas loop at 303 K were performed. A series of purely dispersive *n*-alkane vapour probes (undecane, decane, nonane and octane) and polar probes (ethanol, acetone, ethyl acetate, acetonitrile and dichloromethane) were injected at infinite dilution (4% p/p₀) and V_R^0 was determined using a peak maximum analysis. Methane gas was used as a non-interacting probe giving t_0 for the column, with concentrations of 0.10 p/p₀. Helium was used as the carrier gas at a flow rate of 10.0 standard cubic centimetres per minute for all injections. Duplicate columns were prepared for all samples with a typical column sample packing of 0.7 g. Reproducibility of V_R^0 was typically $\pm 1\%$. The γ_{SV}^d of paracetamol was calculated according to the Schultz *et al.* (20) method using the SMS-iGC analysis software (version 1.2).

Contact Angle Measurement

Sessile drop contact angles were measured using a Krüss Drop Shape Analyser (DSA 10, Krüss GmbH, Hamburg, Germany). Initial drops of about 5 μl were dispensed onto the solid surface. By use of a motor-driven syringe, the volume of the test liquid droplet was slowly increased, allowing the advancing contact angle, θ_a to be determined. The needle remained immersed within the top half of the droplet. The droplet was monitored with a CCD camera and analyzed by the Drop Shape Analysis software (DSA version 1.0, Krüss). The droplet contour is fitted by the tangent method (function $f(x) = a + bx + cx^{0.5} + d/\ln x + e/x^2$ at for both left and right sides of the drop. This curve is then differentiated, and the gradient at the three phase contact point, which defines θ , is calculated. More than 20 contact angle measurements were taken for each liquid on each crystal facet examined. Measurements were obtained in open air at ambient conditions ($T = 20 \pm 2^\circ\text{C}$).

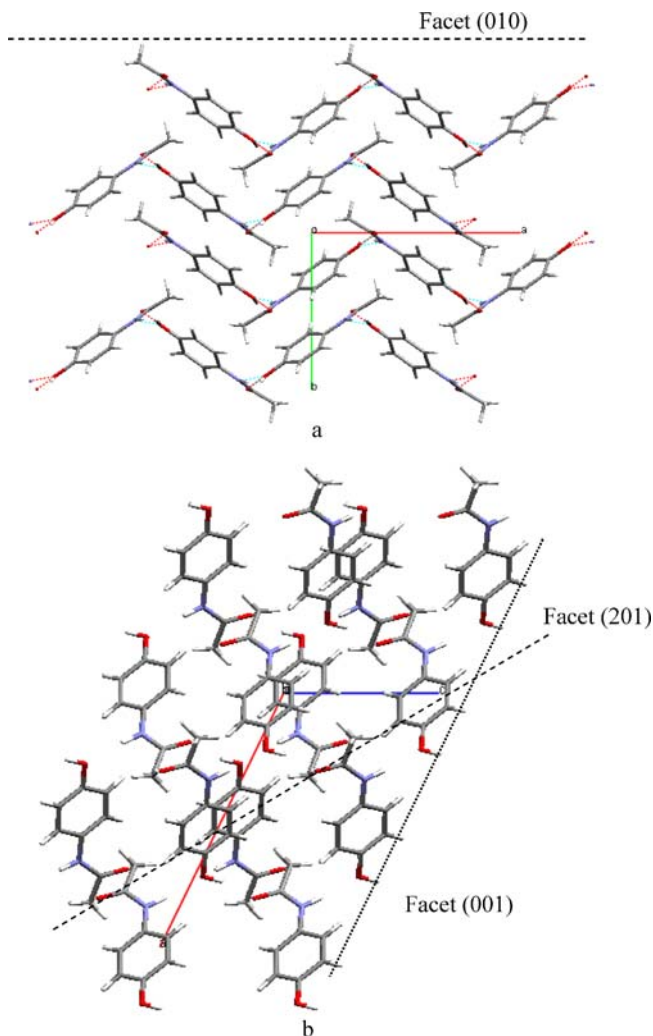


Fig. 3. Molecular structure of (a) facet (010) form I paracetamol along *c*-axis and (b) of facets (001) and (201) form I paracetamol along *b*-axis.

Table IV. γ_{SV}^d of Milled Macroscopic Single Crystals Grown from Saturated Paracetamol in Methanol and Acetone Solution

Particle size (μm)	Milled macroscopic crystal grown from methanol solution	Milled macroscopic crystal grown from acetone solution
32–75	39.6	41.0
75–125	38.9	39.3
125–150	39.3	39.6
150–250	37.8	37.8
250–425	36.6	37.6
425–600	34.8	34.0

RESULTS AND DISCUSSION

Liquid Contact Angle Measurement

Experimental contact angles of probe liquids diiodomethane, water, ethylene glycol and formamide on specific facets of macroscopic single paracetamol form I crystals are shown in Table II. Form I paracetamol crystals exhibit a range of external facets; (201), (001), (011) and (110). The weakest attachment energy plane is parallel to the *b*-axis and is facet (010), which is the preferred fracture plane for this material (29). Differences have been observed for the liquid sessile drop contact angles on the different crystal facets of paracetamol. The detailed anisotropic wetting behaviour for these single crystals is reported elsewhere (26).

On a typical external facet (011), contact angles with diiodomethane of 50° were observed whilst for the cleaved facet (010), a contact angle of 28° was measured. Diiodomethane, a purely dispersive liquid, shows that long-range van der Waals interaction between facet (010) and liquid probe is significantly greater than this liquid's interaction with a typical external facet. This difference is confirmed by the surface energies summarised in Table III which show that the γ_{SV}^d on the (011) external facet was 33.9 mJ/m^2 , whilst the cleaved facet had γ_{SV}^d of 45.1 mJ/m^2 . The contact angles exhibited with water show precisely the opposite trend. For facet (011) a contact angle was found to be 30° whilst for facet (010) the contact angle was greater than 67° . This indicates that cleaved facet (010) is much more hydrophobic than the external face (011) which is confirmed by the polar components of the surface energy of 32.7 and 7.0 mJ/m^2 for faces (011) and (010), respectively.

The crystallographic structure of paracetamol (Fig. 3), not surprisingly, suggests that the different facets may possess different molecular orientation, packing densities and functional groups at the surface. Specifically, this diagram of facet (010) reveals that methyl end groups are present on the surface and as such may account for the much more hydrophobic nature of this facet. The weakest attachment energy plane, facet (010) exposes the hydrophobic methyl groups and at the same time blocks the phenolic OH groups at the surface (14). This surface chemistry yields an overall apolar nature of the surface. The slight polarity of this surface could be due to the aromatic π electrons, which could act as a hydrogen bond acceptor. The paracetamol molecules form a corrugated hydrogen bond sheets held by van der Waals

interactions. At the surface of facet (010), the lack of polar groups and dependence on only the dispersive forces is reflected in the low attachment energy of this facet, and is the preferred cleavage plane (30).

Such significant differences between the surface properties of the cleaved surfaces compared to the external facets leads this work to investigate the effects of milling and different particle size fractions on surface energies of crystalline paracetamol form I.

Dispersive Surface Energy of Milled Crystals

As crystalline materials are milled, resulting in a decrease in particle size, it is reasonable to postulate that the crystals will fracture along their weakest attachment energy facet. This of course is not the only mechanism for fracture, but one would expect it to be the dominant mechanism. For paracetamol, this should result in the exposure of facet (010). The surface chemistry of facet (010) was found to be hydrophobic with a higher γ_{SV}^d from liquid sessile drop contact angle experiments. As such, one can expect the γ_{SV}^d of milled paracetamol to be inversely related to the particle size.

The γ_{SV}^d of the two milled materials as a function of particle size are shown in Table IV. The increasing γ_{SV}^d with a decrease in particle size is observed for both sets of milled samples while γ_{SV}^d was independent of particle size, within experimental error, for unmilled samples as shown in Table V.

The growth of form I paracetamol macroscopic crystals from different solvents, methanol and acetone solution resulted in crystal different habits (Fig. 2). However, similar (within experimental error of $\pm 1 \text{ mJ/m}^2$) γ_{SV}^d values are obtained for same particle size fractions of both sets of milled samples. This indicates that as the particle size is reduced, the crystal fractures preferentially along the weakest attachment energy facet. This fracture results in the weakest attachment energy facet becoming the dominant facet present in the powder. Indeed the γ_{SV}^d values obtained from IGC for the smallest milled size fractions of 39.6 and 41.0 mJ/m^2 are tending towards the 45.1 mJ/m^2 for γ_{SV}^d of the (010) faces as determined by contact angle analysis. Of course, we could only expect that the γ_{SV}^d for the milled materials would approach a value of 45.1 mJ/m^2 , as this value could never be achieved in reality due to the necessary and essential contribution of the other facets present on the milled crystal surface to the average γ_{SV}^d measured. In the case of paracetamol, we know that all of the faces except (010) have a γ_{SV}^d of $34 \pm 0.4 \text{ mJ/m}^2$, therefore we would expect some type of surface area weighted average of

Table V. γ_{SV}^d of Unmilled Single Crystals Grown from Saturated Paracetamol in Methanol and Acetone Solution

Particle size (μm)	Single crystals grown from methanol solution	Single crystals grown from acetone solution
75–150	–	31.26
150–250	33.16	30.67
250–425	35.96	31.20
425–600	33.89	32.32
600–850	33.57	32.91

Table VI. Average γ_{SV}^d of Various Form I Paracetamol Crystals

Facet	γ_{SV}^d
Crystals grown from methanol solution ^a	34.1 ± 1.2
Crystals grown from acetone solution ^a	31.7 ± 0.9
External facets of macroscopic crystals ^b	34.4 ± 0.4

^a Equal average of all particle size fractions.

^b Equal average of all external crystal facets.

γ_{SV}^d between 34 and 45 mJ/m² in magnitude, which is what was observed. It may thus be concluded that surface properties of the milled material are significantly influenced by the weakest attachment energy facet with decreasing particle size. γ_{SV}^d is found to be independent of the starting habit of the macroscopic crystal.

It is however plausible that this increase in γ_{SV}^d might be due to the presence of an amorphous surface zone, as has been reported for milled lactose monohydrate. However, the T_g of paracetamol is approximately 300 K; room temperature. Therefore any amorphous material created during milling, especially at room relative humidity, will have sufficient molecular mobility to quickly crystallised. As the milled samples were normally aged for a couple of weeks prior to measurements, amorphous contributions to surface properties can be safely ruled out in this study. Thus, the increasing values of γ_{SV}^d were consistent with an increasing presence of the (010) facet as the particle size was reduced. There is no reason to expect that aging time post milling should be a factor in the surface energy of crystalline samples as investigated here. However, there is no explicit study on this subject yet published and one cannot fully discount the possibility of a metastable crystal form being created as a result of a high energy milling process. No such evidence was observed in the study reported here.

Dispersive Energy of Unmilled Crystals

The γ_{SV}^d of paracetamol fine crystals grown from different solutions as a function of their particle size are shown in Table V. In the case of the single crystals grown from solution, small differences in γ_{SV}^d are observed for crystals grown from methanol and acetone solutions.

Unlike the milled samples, γ_{SV}^d of both sets of fine crystals grown from methanol and acetone solution were found to be independent of their particle size. This observation is in contrast to the increases in γ_{SV}^d values for the milled sampled with decreasing particle size. Furthermore, for all fine crystal size fractions, the γ_{SV}^d values were lower than those of the milled samples. This reconfirms our view that facet (010) was not initially present in the native crystal, and it is only exposed upon milling.

γ_{SV}^d for the unmilled crystals grown in acetone is marginally lower than γ_{SV}^d for the unmilled crystals grown from methanol. Since the variations in these values are within experimental errors, no additional conclusions are appropriate. However, if one was to speculate, it would be suggested that these slight differences are due to the variations in the shape or habit of these crystals.

The average values for γ_{SV}^d are shown in Table VI for both of the fine and unmilled crystals. These γ_{SV}^d values are however very similar of those obtained by liquid sessile drop contact angle measurements on the external facets of a macroscopic single crystal. γ_{SV}^d of the external facets of paracetamol crystal as measured by contact angles was 34.4 mJ/m² (26).

Acid-Base Contributions of Paracetamol Crystals

The free energy of desorption, ΔG_{AB}° of polar probes; ethanol, acetone, ethyl acetate and acetonitrile were obtained as described in Fig. 1. The acid-base properties of milled and unmilled crystal fractions are found to be dissimilar. ΔG_{AB}° for polar vapour probes on paracetamol crystallised from methanol and acetone and shown in Table VII and Table VIII, respectively. By comparing the values of ΔG_{AB}° and the calculated acid-base numbers, a number of conclusions may be drawn.

The acid-base numbers of milled paracetamol crystal grown from methanol and acetone solution are shown in Figs. 4 and 5. The K_A for milled macroscopic crystals grown from methanol solution was fairly constant with values of 0.11 for the larger fractions, increasing slightly to 0.13 with a reduction in particle sizes. Similarly, for the milled macroscopic crystals from an acetone solution, the K_A for the larger fractions was 0.10 and increasing with decreasing particle

Table VII. Free Energy of Desorption for Paracetamol Crystals Grown From Saturated Methanol Solution

Sample (μm)	Free energy of desorption (kJ mol ⁻¹)			
	Ethanol	Acetone	Ethyl acetate	Acetonitrile
Fine single crystals				
150–250	7.57	6.10	7.62	9.68
250–425	8.68	6.60	8.17	10.30
425–600	6.64	4.93	6.69	8.42
600–850	6.19	5.10	6.67	7.29
Milled macroscopic single crystals				
32–75	10.45	8.13	9.94	11.79
75–125	10.08	8.12	9.79	11.49
125–150	9.93	8.03	9.66	11.46
150–250	9.30	7.57	8.84	11.26
250–425	9.50	7.80	8.72	11.75
425–600	9.33	7.69	8.83	11.61

Table VIII. Free Energy of Desorption for Paracetamol Crystals Grown From Saturated Acetone Solution

Sample (μm)	Free energy of desorption (kJ mol^{-1})			
	Ethanol	Acetone	Ethyl acetate	Acetonitrile
Fine single crystals				
75–150	4.95	4.58	6.23	8.22
150–250	5.86	5.18	6.80	8.36
250–425	7.08	6.05	7.30	9.55
425–600	7.40	6.46	7.49	9.74
600–850	6.73	6.60	5.52	9.04
Milled macroscopic single crystals				
32–75	10.30	7.61	9.96	10.39
75–125	11.14	8.00	9.98	11.89
125–150	10.17	7.29	9.11	10.85
150–250	10.86	7.86	9.49	11.71
250–425	8.17	6.35	7.91	9.79
425–600	9.91	7.27	8.46	11.61

sizes to a maximum value of 0.13. However, a much broader variation in the K_B was found for both samples, with K_B varying from 0.12 to 0.02. The trend was less predictable in both sets of samples, but in general the K_B was lower for the smallest particle sizes fractions.

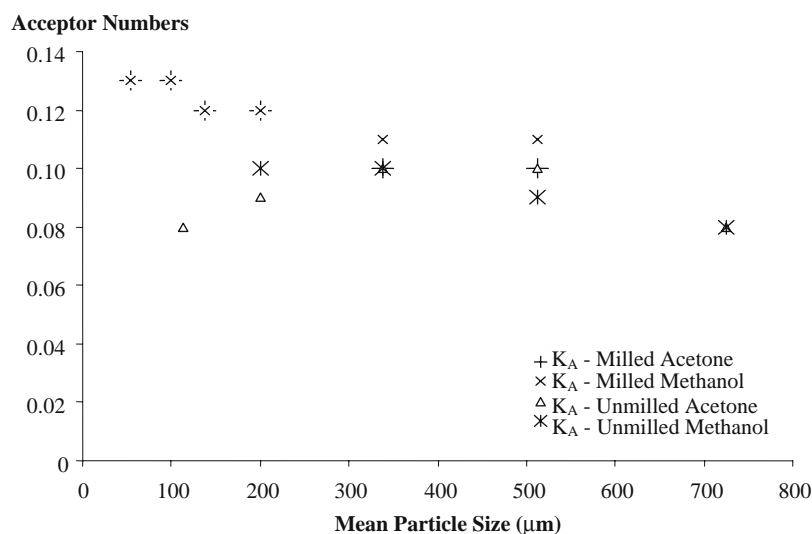
The external facets of paracetamol crystals consist of carbonyl, amine and hydroxyl functionalities in different proportions but contributing to an overall basic nature of the surface. Upon milling, facet (010) is exposed and as this facet lacks the presence of any functional end-groups, with only benzene ring moieties being available on this facet. Contrary to previously published results (14), there are no carbonyl functionalities on facet (010) to give rise to the basic nature of milled crystalline paracetamol as the $-\text{OH}$ appears to form hydrogen bonds with neighbouring amine and carbonyl functionalities, leaving negligible hydrogen bonding potential.

No difference in K_A was noted between the two milled samples confirming that milling exposes an acidic facet (010) while the variability in K_B highlights the potential importance of secondary fracture. For both sets of samples, the

effect of milling on form I paracetamol crystal is found to slightly increase the relatively acidic nature of the material. This indicates an increase in the acidic nature of crystalline paracetamol crystal irrespective of starting habit of the macroscopic crystal.

The K_A and K_B values for the unmilled single crystals grown from methanol and acetone solution are shown in Figs. 4 and 5. These K_A and K_B values are indicative of a more basic contribution resulting in a relatively less acidic powder compared to the milled samples. In unmilled crystals of paracetamol, it is expected that the external facets dominate the surface chemistry of the particulate materials. The external facets of a macroscopic crystal contain carbonyl functionalities which gives rise to the basic nature of the surface.

The correlation between the K_A and K_B values and particle size are however less obvious, for both milled and unmilled samples. The irregular trend in K_B with decreasing particle size (for the milled samples) is thought to be due to the presence of secondary fracture mechanism of the crystal. Though the weakest attachment energy facet (010) will

**Fig. 4.** K_A acceptor numbers for milled macroscopic paracetamol crystals and fine paracetamol crystals as a function of particle size.

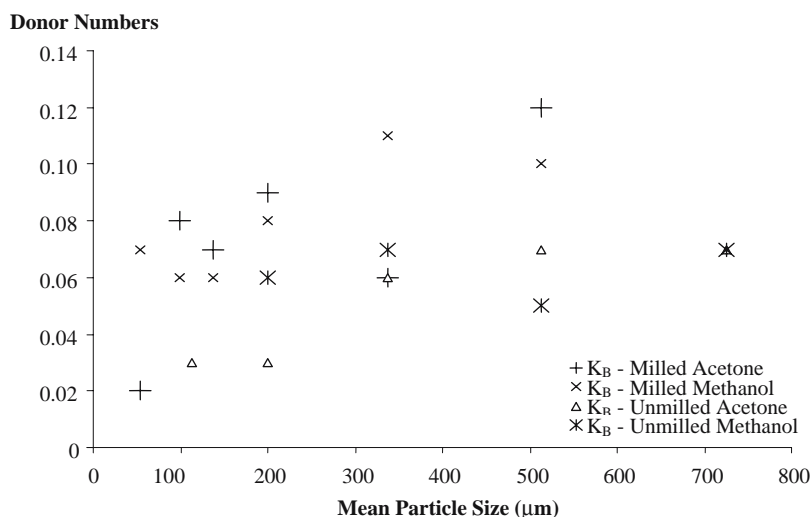


Fig. 5. K_B donor numbers for milled macroscopic paracetamol crystals and fine paracetamol crystals as a function of particle size.

preferentially fracture when force is applied, the fracture of other planes can occur via other secondary fracture processes. As the aspect ratio of the crystal changes, the crystal may preferentially fracture along the (201) or (001) facets for example. This implies that for a crystal plate with sides of facet (010); a fracture exposing facet (201) is preferred if the slab is elongated along b -axis or facet (001) if elongated along c -axis. As such the dependence of K_B on particle size reduction due to milling will be harder to predict. For unmilled samples, the ratio of facet areas (crystal habit) may influence the K_A and K_B trend. The ability to map such surface property heterogeneities is advantageous, and is the focus of another research project within the group.

DISCUSSION

A number of authors have investigated the effects of milling on the surface properties of various solid state pharmaceutical solids including α -lactose monohydrate, propranolol, cefditoren pivoxil and paracetamol (12, 31–33).

In one of the studies, Newell *et al.* (12) focussed on the determination of γ_{SV}^d for a series of α -lactose monohydrate samples prepared via differing routes including milling. They concluded that for a range of amorphous samples, including those whose amorphous content was <1% as induced by milling, all had a γ_{SV}^d which was at least 20% greater than the unmilled crystalline samples of α -lactose monohydrate. These results were consistent with the view that an amorphous state was a higher energy state than the equilibrium crystal system. Milled samples without a measurable amorphous content were not available in this study, thus the effect of particle size on γ_{SV}^d for differing pure crystalline materials could not be assessed.

However, York *et al.* (16) have considered this in their work on DL-propranolol hydrochloride. They found that decreasing the particle size from 75 to 6.6 μm resulted in an increase in 40% in γ_{SV}^d . The authors also reported that as particle size decreased, a modest increase in surface basicity and a modest decrease in surface acidity. They argued that

the most likely fracture plan was the (101) facet which is dominated by naphthalene rings. The presence of these groups on the surface could account for the increased basicity following milling.

Trowbridge *et al.* (33) reported a similar trend on the milling of paracetamol. They reported a 20% increase in γ_{SV}^d with particle size decreasing from 30 to 10 μm . They observed that as particle size decreased, surface basicity increased and surface acidity decreased. This could be argued to be consistent with the expected fracture in paracetamol of the (010) plane, with decreases in acidity and increases in basicity associated with this surface.

In both of these studies, the workers reported a maximum for γ_{SV}^d of $60 \pm 1 \text{ mJ/m}^2$, a rather high value for an organic solid. The authors concluded that surface energy was apparently independent of particle size, once below a critical particle size of approximately 10 μm .

Ohta and Buckton have reported on the surface properties of milled cefditoren pivoxil as determined using IGC (32). They observed that there was an initial increase in γ_{SV}^d after an initial 1-min milling period. Thereafter, γ_{SV}^d decreased with increasing milling time. It is significant to note that this material has a propensity to transform into an amorphous form and indeed after 30 min milling, this material is over 90% amorphous. The authors also reported that the particle size did not depend upon milling time, with a typical post milling particle diameter of 8–9 μm , having started with an initial mean diameter of 16.5 μm . Using acid-base probes the authors went onto conclude that their material became increasingly basic as the milling proceeds, and that this trend agreed with the trend in decreasing crystallinity. They ascribed this basicity change to the increasing donor properties of the carbonyl groups in the amorphous cefditoren pivoxil.

The work presented here illustrates some of the complexities associated with the surface property changes associated with milling. As well as the previously established importance of surface amorphous zones that may be present on particle surfaces, the importance of specific crystalline morphological facets is shown to be important in the current

work. It is important to note that the methods of particle manufacture, either growth from native solution, or preparation by milling, can have a real and measurable effect on surface properties, especially γ_{SV}^d . Therefore surface properties can vary with particle size as clearly shown for the case of the milled material. Thus, particle size variations can have a direct relationship to surface energy variations as shown here for paracetamol form I, which in turn is related to the anisotropic surface properties of crystalline pharmaceutical solids (26).

It is possible to summarise that variations, indeed heterogeneity, in the surface energy of fine pharmaceutical powders can depend upon:

- intrinsic anisotropic surface energetics of crystalline solids
- presence of surface amorphous zones and their surface energy
- effect of processing operations on the prevalence of amorphous zones
- surface area population or distribution for specific crystalline facets, as determined by the processing history of the solid.

In light of the common experiences of batch to batch variations in milling of powders, dry powder inhalator performance and other reliability issues on powder processing, as well as our observations reported here, it is concluded that important variations or heterogeneity in the surface properties of milled materials are probably the norm rather than the exception.

CONCLUSIONS

The surface energetics of milled crystalline paracetamol form I powders was found to be representative of the weakest attachment energy facet (010), which exhibited the largest γ_{SV}^d . Consequently, γ_{SV}^d increased with decreasing particle size due to the milling induced exposure of the (010) facet. The γ_{SV}^d of milled materials were also found to be independent of the starting macroscopic crystal habit. In unmilled single crystals, the γ_{SV}^d was lower compared to the milled samples and representative of the energetics of the external facets of a single crystal. These measurements of γ_{SV}^d were in good agreement with contact angle measurements by liquid sessile drop methods.

The exposure of the weakest attachment energy facet during the milling of macroscopic crystals gave rise to an acidic nature of milled materials. The K_A of the milled materials were found to be fairly consistent while the K_B may be indicative of the secondary fracture of the crystalline material. An overall increase in the relative acidity was found due to milling, as a change in surface functionalities is proposed when the dominance of external facets are replaced by the (010) facet. In unmilled paracetamol crystal, the presence of carbonyl functionalities on the external facets contributed to the basic character. The habit of planar crystals with dominant (201) facets was seen to be more basic than the prismatic crystals.

The unmilled single crystals exhibited properties reflective of the native external facets of paracetamol crystal and

the effect of milling on a form I paracetamol crystal exposes a hydrophobic surface with increasing contribution as particle size is reduced.

REFERENCES

1. R. C. Rowe. Correlation between predicted binder spreading coefficients and measured granule and tablet properties in the granulation of paracetamol. *Int. J. Pharm.* **58**:209–213 (1990).
2. G. Buckton. Assessment of the wettability of pharmaceutical powders. In: K. L. Mittal (ed.), *Contact Angle, Wettability and Adhesion*, VSP, Utrecht, The Netherlands, 1993, pp. 437–451.
3. D. Winn and M. F. Doherty. Modeling crystal shapes of organic materials grown from solution. *AIChE J.* **46**:1348–1367 (2000).
4. V. Chikhalia, R. T. Forbes, R. A. Storey, and M. Ticehurst. The effect of crystal morphology and mill type on milling induced crystal disorder. *Eur. J. Pharm. Sci.* **27**:19–26 (2006).
5. T. Young. An essay on the cohesion of fluids. *Philos. Trans. R. Soc. Lon.* **95**:65–87 (1805).
6. D. Williams. Inverse gas chromatography. In: H. Ishida (ed.), *Characterisation of Composite Materials*, Butterworth-Heinemann, London, 1994, pp. 80–104.
7. F. Thielmann. Introduction into the characterisation of porous materials by inverse gas chromatography. *J. Chromatogr. A* **1037**:115–123 (2004).
8. J. R. Conder and C. L. Young. *Physicochemical Measurement by Gas Chromatography*, Wiley, Chichester, 1979.
9. A. V. Kiselev and Y. I. Yashin. *Gas-Adsorption Chromatography*, Plenum, London, 1969.
10. E. Papirer and H. Balard. E. Pefferkorn (ed.), *Interfacial Phenomena in Chromatography*, Marcel Dekker, New York, 1999.
11. H. E. Newell, G. Buckton, D. A. Butler, F. Thielmann, and D. R. Williams. The use of inverse phase gas chromatography to study the change of surface energy of amorphous lactose as a function of relative humidity and the processes of collapse and crystallisation. *Int. J. Pharm.* **217**:45–56 (2001).
12. H. E. Newell, G. Buckton, D. A. Butler, F. Thielmann, and D. R. Williams. The use of inverse gas chromatography to measure the surface energy of crystalline, amorphous and recently milled lactose. *Pharm. Res.* **18**:662–666 (2001).
13. I. M. Grimsey, J. C. Feeley, and P. York. Analysis of the surface energy of pharmaceutical powders by inverse gas chromatography. *J. Pharm. Sci.* **91**:571–583 (2002).
14. I. M. Grimsey, J. C. Osborn, S. W. Doughty, P. York, and R. C. Rowe. The application of molecular modelling to the interpretation of inverse gas chromatography data. *J. Chromatogr. A* **969**:49–57 (2002).
15. M. D. Ticehurst, R. C. Rowe, and P. York. Determination of the surface properties of two batches of salbutamol sulphate by inverse gas chromatography. *Int. J. Pharm.* **111**:241–249 (1994).
16. P. York, M. D. Ticehurst, J. C. Osborn, R. J. Roberts, and R. C. Rowe. Characterisation of the surface energetics of milled dl-propranolol hydrochloride using inverse gas chromatography and molecular modelling. *Int. J. Pharm.* **174**:179–186 (1998).
17. J. Y. Y. Heng, D. F. Pearse, D. A. Wilson, and D. R. Williams. Characterization of solid state materials using vapor sorption methods. In: A. Zakrzewski and M. Zakrzewski (eds.), *Solid State Characterization of Pharmaceuticals*, ASSA, Danbury Connecticut, 2006.
18. G. Buckton. Characterisation of small changes in the physical properties of powders of significance for dry powder inhaler formulations. *Adv. Drug Deliv. Rev.* **26**:17–27 (1997).
19. F. M. Fowkes. Attractive forces at interfaces. *Ind. Eng. Chem.* **56**:40–52 (1964).
20. J. Schultz, L. Lavielle, and C. Martin. The role of the interface in carbon fibre-epoxy composites. *J. Adhes.* **23**:45–60 (1987).
21. G. M. Dorris and D. G. Gray. Adsorption of *n*-alkanes at zero surface coverage on cellulose paper and wood fibers. *J. Colloid Interface Sci.* **77**:353–362 (1980).

22. U. Panzer and H. P. Schreiber. On the evaluation of surface interactions by inverse gas chromatography. *Macromolecules* **25**:3631–3633 (1992).
23. V. Gutmann. Coordination chemistry of certain transition-metal ions. The role of solvent. *Coord. Chem. Rev.* **2**:239–256 (1966).
24. F. L. Riddle and F. M. Fowkes. Spectral shifts in acid-base chemistry. I. van der Waals contribution to acceptor numbers. *J. Am. Chem. Soc.* **112**:3259–3264 (1990).
25. J. W. Mullin. *Crystallization*. 3rd ed. Butterworth-Heinemann, Oxford, 1993.
26. J. Y. Y. Heng, A. Bismarck, A. F. Lee, K. Wilson, and D. R. Williams. Anisotropic wettability of macroscopic form I paracetamol crystals. *Langmuir* **22**:2760–2769 (2006).
27. E. M. Ålander, M. S. Uusi-Penttilä, and Å. C. Rasmuson. Agglomeration of paracetamol during crystallization in pure and mixed solvents. *Ind. Eng. Chem. Res.* **43**:629–637 (2004).
28. R. I. Ristic, S. Finnie, D. B. Sheen, and J. N. Sherwood. Macro- and micromorphology of monoclinic paracetamol grown from pure aqueous solution. *J. Phys. Chem. B* **105**:9057–9066 (2001).
29. W. C. Duncan-Hewitt, D. L. Mount, and A. Yu. Hardness anisotropy of acetaminophen crystals. *Pharm. Res.* **11**:616–623 (1994).
30. G. Nichols and C. S. Frampton. Physicochemical characterization of the orthorhombic polymorph of paracetamol crystallized from solution. *J. Pharm. Sci.* **87**:684–693 (1998).
31. I. M. Grimsey, J. C. Feeley, and P. York. Analysis of the surface energy of pharmaceutical powders by inverse gas chromatography. *J. Pharm. Sci.* **91**:571–583 (2002).
32. M. Ohta and G. Buckton. Determination of the changes in surface energetics of cefditoren pivoxil as a consequence of processing induced disorder and equilibration to different relative humidities. *Int. J. Pharm.* **269**:81–88 (2004).
33. L. Trowbridge, I. M. Grimsey, and P. York. Influence of milling on the surface properties of acetaminophen. *AAPS PharmSci (Suppl.)*(1):310 (1998).